Volume 2 | Number 36 | 28 September 2014 | Pages 14741–15210

Journal of Materials Chemistry A

Materials for energy and sustainability

www.rsc.org/MaterialsA

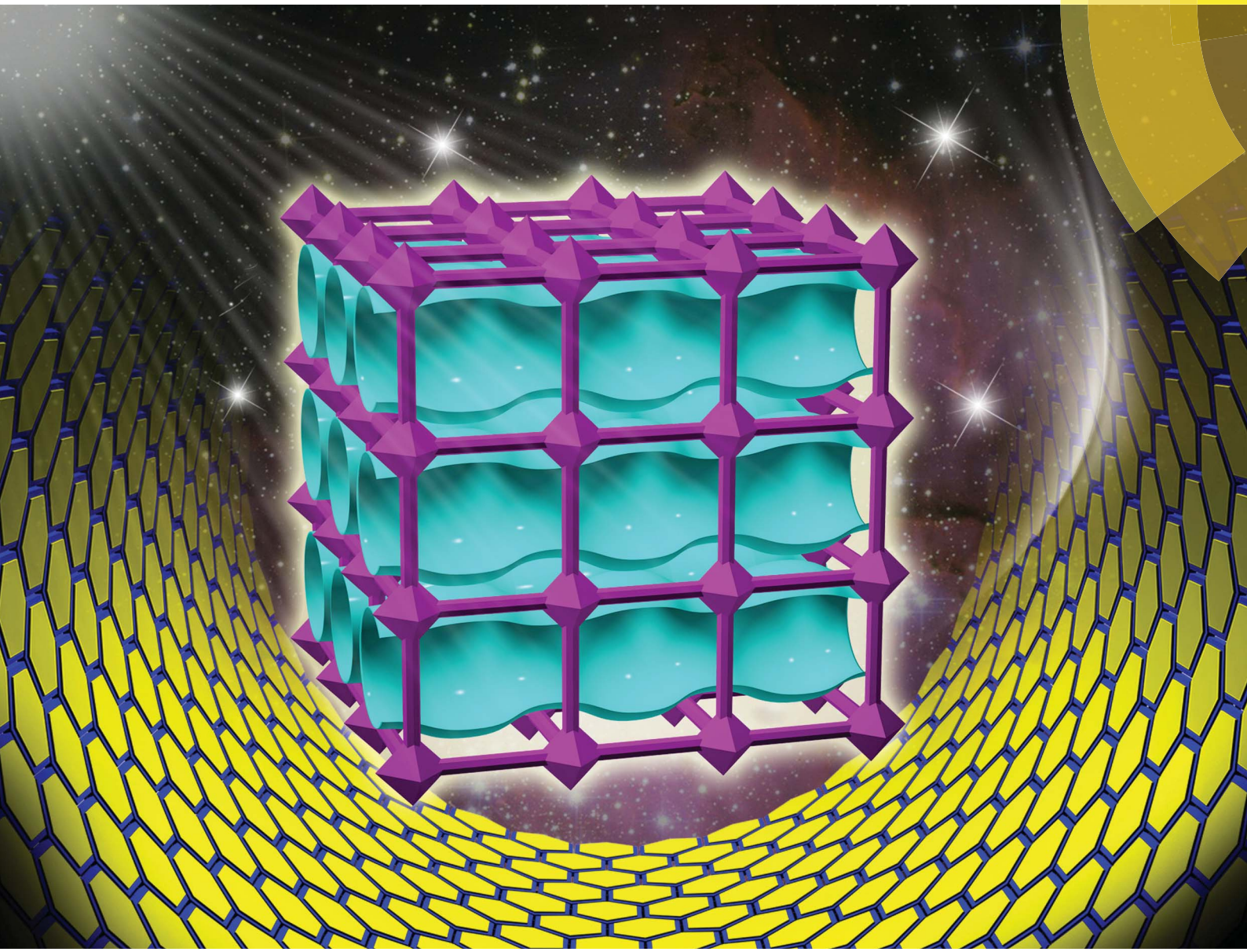

ISSN 2050-7488

ROYAL SOCIETY OF CHEMISTRY

PAPER

Chao Qin, Zhong-Min Su, Fu-Chen Liu *et al.*

Controllable synthesis of isoreticular pillared-layer MOFs: gas adsorption, iodine sorption and sensing small molecules

Journal of Materials Chemistry A

PAPER

View Article Online
View Journal | View Issue

Cite this: J. Mater. Chem. A, 2014, 2, 14827

Controllable synthesis of isoreticular pillared-layer MOFs: gas adsorption, iodine sorption and sensing small molecules†

Xiao-Li Hu,[a] Fu-Hong Liu,[a] Hai-Ning Wang,[a] Chao Qin,*[a] Chun-Yi Sun,[a] Zhong-Min Su*[a] and Fu-Chen Liu*[b]

Received 10th April 2014
Accepted 27th June 2014

DOI: 10.1039/c4ta01749h

www.rsc.org/MaterialsA

Five isostructural pillared-layer MOFs (metal–organic frameworks) have been constructed by selection of layers and size-alterable pillar ligands. These MOFs show similar structures but different interlayer distances, pore volumes and pore surface functionalizations depending on the lengths and functions of pillar ligands. **1–5** display a certain degree of framework stabilities, and also exhibit CO_2 uptakes. In addition, **1** can serve as a host for encapsulating I_2 and exhibit an outstanding performance in reversible adsorption of iodine molecules. Furthermore, **1–5** can be used to separate dye molecules based on the size-exclusion effect and **3** can be employed as a column-chromatographic filler to separate Rhodamine B (RB) and Methylene Blue (MB).

Introduction

Metal–organic frameworks (MOFs) have attracted tremendous attention in recent years and are being evaluated for diverse potential applications in gas adsorption, catalysis and selective separation.[1–4] These functions mainly depend on the pore characteristics of MOFs, including pore size and shape. Thus, the design and prediction of the MOF structure are critical for the construction of MOFs with desired properties and characteristics.[5] However, the controllable synthesis of MOFs still remains one of the most compelling challenges for chemists. Much effort has been dedicated to achieving MOFs with tunable pore sizes from micropore to mesopore. Employing size-alterable organic linkers to systematically modulate pore size and shape, is one of the most commonly used strategies.[6] As an important branch of MOFs, pillared-layer structures have proved to be an efficient route to controllably construct frameworks.[7,8] In this way, the structures of a wide variety of MOFs can be predicted and systematically designed. Moreover, chemical functionality of the open frameworks such as hydrophilic/hydrophobic character, hydrogen bonding, and open metal site can be easily controlled *via* modification of the pillars.[9] Also, flexible pillars can be used for designing and preparing dynamic porous MOFs that can both shrink and expand in response to the presence and absence of guest molecules.[10]

Dyes are widely used in many industries such as paper, textiles, printing, plastics, cosmetics, and pharmaceuticals.[11] The discharge of dyes into water has received considerable attention because of their overall environmental hazards. Usually, the dyes in water are difficult to degrade because of their poor biodegradability and complex structures.[12] From an environmental point of view, the removal of dyes from effluents before discharge into natural bodies is extremely important. So far, numerous methods have been developed for the removal of dyes from an aqueous environment.[13] The common adsorbents primarily include activated carbons, zeolites, biomass, clays and so on.[12] However, MOFs as potential adsorbents have received less attention.

We firstly employed 1,2,4-triazole and NH_2bdc (amino-1,4-benzenedicarboxylate) ligands to successfully achieve **2**. To ensure formation of a series of pillared-layer MOFs, **2** was functionalized with organic groups –Br, $-C_6H_5$ and its pore size was altered with the molecular struts CH=CH and diphenyl oxide. With progressively longer links fma (fumaric acid), NH_2bdc to oba (4,4′-oxybis(benzoate)), the interlayer distances of **1**, **2**, and **5** incrementally varied from 9.6, 11.7 to 17.1 Å. They show different dye absorption capacities because of different pore volumes resulting from size-alterable ligands.

Experimental

Materials and physical measurements

All chemical materials were purchased from commercial sources and used without further purification. The FT-IR spectra

[a]Institute of Functional Material Chemistry, Key Laboratory of Polyoxometalate Science of Ministry of Education, Northeast Normal University, Changchun, 130024 Jilin, P. R. China. E-mail: qinc703@nenu.edu.cn; zmsu@nenu.edu.cn; Fax: +86-431-85684009; Tel: +86-431-85099108

[b]School of Chemistry and Chemical Engineering, Tianjin University of Technology, Tianjin, 300384, P. R. China. E-mail: fuchenliutj@yahoo.com

† Electronic supplementary information (ESI) available: XRPD, TG, isosteric heats spectra, UV/vis spectra, photoluminescence spectra and additional figures. CCDC-945490 (**1**), 945492 (**2**), 945493 (**3**), 945494 (**4**), and 945495 (**5**). For ESI and crystallographic data in CIF or other electronic format see DOI: 10.1039/c4ta01749h

were recorded from KBr pellets in the range 4000–400 cm^{-1} on a Mattson Alpha-Centauri spectrometer. XRPD patterns were recorded on a Siemens D5005 diffractometer with Cu Kα (λ = 1.5418 Å) radiation in the range of 3–60° at a rate of 5° min^{-1}. The UV/vis absorption spectra were examined on a Shimadzu UV-2550 spectrophotometer in the wavelength range of 200–800 nm. The C, H, and N elemental analyses were conducted on a Perkin-Elmer 2400CHN elemental analyzer. TG curves were performed on a Perkin-Elmer TG-7 analyzer heated from room temperature to 1000 °C at a ramp rate of 5 °C min^{-1} under nitrogen. The photoluminescence spectra were measured on a Perkin-Elmer FLS-920 Edinburgh Fluorescence Spectrometer.

Preparation of $C_{13}H_{19}N_7O_6Zn_2$ (1)

A mixture of $Zn(NO_3)_2\cdot 6H_2O$ (60 mg, 0.2 mmol), 1,2,4-triazole (14 mg, 0.2 mmol), and fma (14 mg, 0.1 mmol) was dissolved in 6 mL of DMA (*N*,*N*-dimethylacetamide)–MeOH (methanol) (1 : 1, v/v). The final mixture was placed in a Parr Teflon-lined stainless steel vessel (15 mL) under autogenous pressure and heated at 100 °C for 3 days. Colorless crystals were obtained, which were washed with mother liquid, and dried under ambient conditions. Elemental analysis: anal. calcd for $C_{13}H_{19}N_7O_6Zn_2$: C 31.22; H 3.83; N 19.60%. Found: C 31.23; H 3.80; N 19.62%. IR (KBr, cm^{-1}): 917.27 (w), 2939.87 (w), 805.24 (w), 475.97 (w), 3099.31 (w), 1039.13 (w), 984.09 (w), 590.97 (w), 1216.71 (w), 3446.43 (m), 1007.29 (m), 1169.45 (m), 705.63 (m), 1299.53 (m), 1522.98 (s), 1091.91 (s), 667.63 (s), 1398.55 (s), 1591.53 (s).

Preparation of $C_{17}H_{22}N_8O_6Zn_2$ (2)

The synthetic procedure is similar to that of **1** except that fma was replaced by NH_2bdc. $Zn(NO_3)_2\cdot 6H_2O$ (60 mg, 0.2 mmol), 1,2,4-triazole (14 mg, 0.2 mmol), and NH_2bdc (18 mg, 0.1 mmol) were dissolved in 6 mL of DMA–MeOH (1 : 1, v/v). The final mixture was placed in a Parr Teflon-lined stainless steel vessel (15 mL) under autogenous pressure and heated at 100 °C for 3 days. Colorless crystals were obtained, which were washed with mother liquid, and dried under ambient conditions. Elemental analysis: anal. calcd for $C_{17}H_{22}N_8O_6Zn_2$: C 36.13; H 3.92; N 19.83%. Found: C 36.15; H 3.90; N 19.80%. IR (KBr, cm^{-1}): 2482.90 (w), 704.90 (w), 3024.38 (w), 2933.65 (w), 922.51 (w), 474.17 (w), 816.50 (w), 891.30 (w), 3349.74 (w), 3468.22 (w), 588.49 (w), 3099.05 (w), 848.18 (w), 770.82 (m), 1214.62 (m), 1457.37 (m), 1307.27 (m), 1263.56 (m), 1389.83 (m), 1007.77 (m), 666.29 (s), 1085.64 (s), 1164.96 (s), 1517.23 (s), 1570.23 (s), 1624.15 (s).

Preparation of $C_{17}H_{20}N_7O_6BrZn_2$ (3)

The synthetic procedure is similar to that of **1** except that fma was replaced by Brbdc (bromo-1,4-benzenedicarboxylate). $Zn(NO_3)_2\cdot 6H_2O$ (60 mg, 0.2 mmol), 1,2,4-triazole (14 mg, 0.2 mmol), and Brbdc (24 mg, 0.1 mmol) were dissolved in 6 mL of DMA–MeOH (1 : 1, v/v). The final mixture was placed in a Parr Teflon-lined stainless steel vessel (15 mL) under autogenous pressure and heated at 100 °C for 3 days. Colorless crystals were obtained, which were washed with mother liquid, and dried under ambient conditions. Elemental analysis: anal. calcd for $C_{17}H_{20}N_7O_6BrZn_2$: C 32.46; H 3.20; N 15.59%. Found: C 32.42; H 3.22; N 15.55%. IR (KBr, cm^{-1}): 3031.67 (w), 2936.11 (w), 475.43 (w), 3612.72 (w), 3443.61 (w), 918.39 (w), 586.53 (w), 1723.68 (w), 3100.03 (w), 770.76 (w), 841.36 (w), 1037.39 (w), 1217.73 (w), 1478.90 (w), 1007.56 (m), 1300.21 (m), 1523.48 (m), 1168.56 (m), 1090.59 (s), 667.24 (s), 1373.71 (s), 1623.82 (s).

Preparation of $C_{21}H_{23}N_7O_6Zn_2$ (4)

The synthetic procedure is similar to that of **1** except that fma was replaced by 1,4-ndc (1,4-naphthalenedicarboxylate). $Zn(NO_3)_2\cdot 6H_2O$ (60 mg, 0.2 mmol), 1,2,4-triazole (14 mg, 0.2 mmol), and 1,4-ndc (21 mg, 0.1 mmol) were dissolved in 6 mL of DMA–MeOH (1 : 1, v/v). The final mixture was placed in a Parr Teflon-lined stainless steel vessel (15 mL) under autogenous pressure and heated at 100 °C for 3 days. Colorless crystals were obtained, which were washed with mother liquid, and dried under ambient conditions. Elemental analysis: anal. calcd for $C_{21}H_{23}N_7O_6Zn_2$: C 42.02; H 3.86; N 16.33. Found: C 42.00; H 3.90; N 16.32. IR (KBr, cm^{-1}): 3028.29 (w), 2933.41 (w), 589.42 (w), 3483.03 (w), 843.05 (w), 1259.74 (w), 1037.31 (w), 1219.44 (w), 3093.49 (w), 1457.92 (m), 1006.07 (m), 1664.19 (m), 794.25 (m), 1169.57 (m), 669.20 (m), 1300.76 (m), 1524.18 (s), 1362.69 (s), 1091.11 (s), 1566.98 (s), 1394.49 (s), 1622.57 (s).

Preparation of $C_{26}H_{30}N_8O_7Zn_2$ (5)

A mixture of $Zn(NO_3)_2\cdot 6H_2O$ (60 mg, 0.2 mmol), 1,2,4-triazole (14 mg, 0.2 mmol), and H_2oba (25.8 mg, 0.1 mmol) was dissolved in 6 mL of DMA–MeOH–H_2O (1 : 1 : 2, v/v/v). The final mixture was placed in a Parr Teflon-lined stainless steel vessel (15 mL) under autogenous pressure and heated at 100 °C for 3 days. Colorless crystals were obtained, which were washed with mother liquid, and dried under ambient conditions. Elemental analysis: anal. calcd for $C_{26}H_{30}N_8O_7Zn_2$: C 44.78; H 4.34; N 16.07%. Found: C 44.80; H 4.32; N 16.08%. IR (KBr, cm^{-1}): 474.14 (w), 629.14 (w), 516.54 (w), 698.03 (w), 802.83 (w), 843.49 (w), 590.73 (w), 434.30 (w), 768.13 (w), 2935.18 (m), 3477.63 (m), 1037.05 (m), 880.00 (m), 783.59 (m), 3099.41 (m), 1008.20 (m), 1300.10 (m), 1523.71 (s), 1560.99 (s), 1091.02 (s), 1161.85 (s), 667.56 (s), 1249.45 (s), 1394.78 (s), 1602.08 (s).

Single crystal X-ray diffraction

Single-crystal X-ray diffraction data for **1–5** were recorded on a Bruker Apex CCD II area-detector diffractometer with graphite monochromated Mo-Kα radiation (λ = 0.71073 Å) at 296(2) K. Absorption corrections were applied using the multi-scan technique. Their structures were solved by the direct method of SHELXS-97 and refined by full-matrix least-square techniques with the SHELXL-97 program.[14] Because guest molecules in the channels of **1–5** were highly disordered and could not be modeled properly, the SQUEEZE routine of PLATON was applied to remove their contributions to the scattering.[15] The reported refinements are of the guest-free structures obtained by the SQUEEZE routine, and the results were attached to the CIF file. The crystal data and structure refinement results of **1–5** are summarized in Table S1.†

Gas sorption experiments

The N_2 and CO_2 sorption measurements were performed on automatic volumetric adsorption equipment (Belsorp mini II). Before gas adsorption measurements, the samples were immersed in CH_2Cl_2 for 24 h, and the extracts were decanted. Fresh CH_2Cl_2 was subsequently added, and the crystals were allowed to stay for an additional 24 h to remove the nonvolatile solvates (DMA). After the removal of dichloromethane by decanting, the samples were activated by drying under a dynamic vacuum at room temperature over night. Before the measurement, the samples were dried again by using the "outgas" function of the surface area analyzer for 12 h at 90 °C. Meanwhile, the activated samples **1a** were immersed in water, HCl (pH = 2) and NaOH (pH = 12) solutions. After the removal of water by decanting, the samples **1a** were tested for N_2 sorption measurements.

Iodine sorption experiments

The fresh samples of **1** (80 mg) were immersed in a hexane (3 mL) solution of I_2 (0.01 mol L^{-1}), to give I_2@**1**. The photographs were used to determine the adsorption ability. The crystals of I_2@**1** (10 mg) were soaked in dry ethanol (5 mL) and UV/vis spectra and photographs were used to determine the desorption ability.

Dye adsorption and separation

Freshly prepared **1–5** (20 mg) were transferred to aqueous solutions (8 mL) of Methylene Blue (MB), Rhodamine B (RB), Methyl Orange (MO) and Congo Red (CR), respectively, in 10 mL sealed glass bottles. Meanwhile, freshly prepared **1**, **2**, and **5** were transferred to aqueous solutions (8 mL) of mixtures of Methylene Blue (MB) and Rhodamine B (RB) in 10 mL sealed glass bottles. UV/vis spectra and photographs were used to determine the selective adsorption ability of **1**, **2**, and **5** after time intervals.

Dye release

1, **2** and **5** loaded with dye molecules were transferred to pure MeOH solution (5 mL) in 10 mL sealed glass bottles. UV/vis spectra were used to determine the selective release of **1–5** after time intervals.

Results and discussion

Synthesis and crystal structures

The molecular structures of **1–5** were determined by X-ray crystallography. The crystallographic parameters of these compounds are given in Table S1.† **1–5** are all pillared-layer structures based on the Zn-triazolate layers and dicarboxylate pillars. Two-dimensional layers of {Zn(trz)} are formed in the *ac* plane, which are connected by pillar ligands for five crystalline products, namely, $[Zn_2(trz)_2(L)\cdot DMA\cdot MeOH]_n$ [L = fma, **1**; NH_2bdc, **2**; Brbdc, **3**; 1,4-ndc, **4**], and $[Zn_2(trz)_2(oba)\cdot 2DMA]_n$ (**5**).

Single-crystal structure analysis reveals that **1** crystallizes in the tetragonal system, space group *P*4/*ncc*. As shown in Fig. 1a, the asymmetric unit of **1** contains one Zn atom, one-half of the fma ligand and one 1,2,4-triazole ligand. The Zn ion is five coordinated in a distorted trigonal-bipyramidal geometry with three nitrogen atoms from three triazole ligands and two carboxylate oxygen atoms from the fma ligand (Zn–N 2.006 Å, Zn–O 1.960 Å). Each triazole ligand binds to three Zn atoms through 1,2,4-position N atoms and the connection of triazole and the Zn ion resulted in a two-dimensional (2D) layer with 4.8^2 topology. The adjacent {Zn(trz)} layers are further connected by the fma pillars to give rise to an overall 3D pillared-layer structure. Interestingly, the network contains channels running along the *a*, *b* and *c* axes. PLATON calculations show that the effective pore volume for **1** is about 52% (2214.4 $Å^3$) per unit cell (4261.4 $Å^3$), which is occupied by solvent molecules.[16] **5** has a similar pillared-layer structure to **1**, with the replacement of fma ligands by the longer carboxylate ligands oba. And both the entrance of the channels and the interlayer distance are enlarged. For the channels along the *b* axis, the dimensions of channels for **1**, **2** and **5** have the sizes ranging from 9.6 Å × 6.5 $Å^2$, 11.7 Å × 6.5 $Å^2$ to 17.1 × 6.5 $Å^2$ (*a* × *c*) (Fig. S1†). Viewed along the *c* axis, **1–5** have the same channel dimension of 6.5 × 6.5 $Å^2$ (*a* × *b*) because of the same {Zn(trz)} layers. Meanwhile, **3** and **4** have the same structures as **2**, with benzene rings functionalized with the substituent groups –Br, and $-C_6H_5$. Notably, the uncoordinated functional groups of ligands are directed into the rectangular pores. Topologically, regarding the {Zn(trz)} unit as a 6-connected node and dicarboxylate as the linker, the 3D structures of **1–5** can be simplified as isostructural pcu topologies. The pcu topology is a primitive cubic lattice net with Schläfli symbol ($4^{12}6^3$), such as NaCl and α-po.[17]

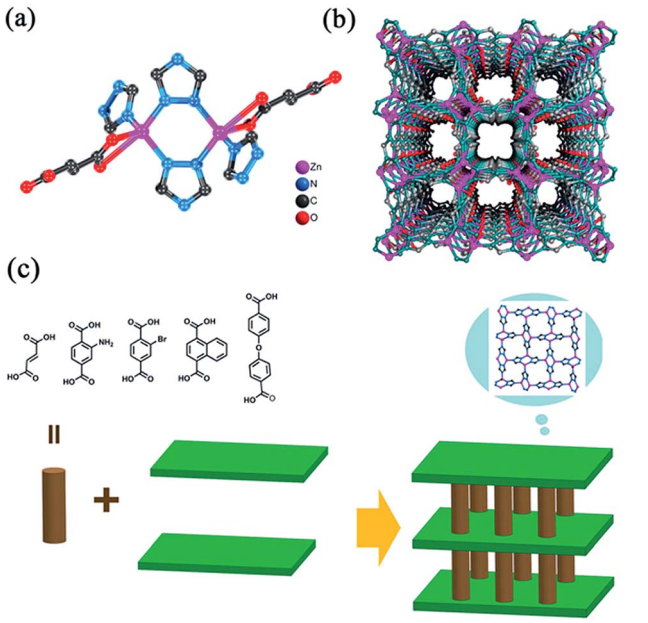

Fig. 1 (a) The coordination environment of the Zn(II) center in **1**. The hydrogen atoms are omitted for clarity (Zn, pink; N, blue; C, gray; O, red). (b) 3D framework of **1** along the *c* axis. (c) Schematic representations of **1–5** structures and view of the wave-like 2D sheet by trz and Zn ions along the *c* axis.

Thermal and chemical stability

The purities of the as-synthesized **1–5** were confirmed by similarities between simulated and experimental X-ray powder diffraction (XRPD) patterns (Fig. S2†). The TG curve of **2** reveals a weight loss of 20.9% from 50 to 280 °C, in agreement with the weight of DMA and CH_3OH molecules (calcd 21.0%). The TG curve indicates that **2** can be thermally stable around 350 °C (Fig. S3†). As we know, a good gas storage (or separation) material must be stable toward moisture in practical applications.[18] Thus, we examined their stability to show whether these materials will be useful in practical applications. After soaking **1–5** in water for 24 h at ambient temperature and 100 °C, their XRPD patterns keep the same peak positions although their solid samples become not too transparent (Fig. S4†). In addition, their ability to resist acid and alkali solutions was also investigated. Apart from **4** that become floccule in hydrochloric acid solution, other four MOFs are stable in both hydrochloric acid solution (pH = 2) and sodium hydroxide solution (pH = 12), as confirmed by the XRPD patterns of these samples (Fig. S5†). More remarkably, even after exposure to air for three months, their XRPD patterns have similar shape and intensity.

Gas adsorption properties

To study the porosity of compounds, N_2 and CO_2 adsorption studies were performed. The activated samples were prepared by exchanging the solvent in the as-synthesized **1–5** with CH_2Cl_2, followed by evacuation under vacuum. Samples of **1–5** were evacuated under vacuum at room temperature overnight to completely remove the solvent CH_2Cl_2 molecules and thus to form guest-free phases **1a–5a**. The XRPD patterns of **1a–5a** show that the broadened peaks keep the positions, indicating the maintenance of the frameworks (Fig. S2†).

The architectural stability and permanent porosity of **1a–3a** were confirmed by performing the N_2 adsorption experiments at 77 K, displaying type I adsorption isotherms characteristic of microporous solids. The nitrogen adsorptions showed good reversibility. The N_2 adsorption amounts of **1a–3a** at 1 bar were about 118.5, 150.3, and 158.2 $cm^3\ g^{-1}$, which correspond to 21.2, 30.3, and 35.6 N_2 per cell (Fig. 2). For **1a–3a**, the apparent BET areas were 363, 453, and 506 $m^2\ g^{-1}$, based on the nitrogen adsorption isotherms. The total pore volumes were 0.212, 0.320, and 0.245 $cm^3\ g^{-1}$, lower than the theoretical pore volume calculated by PLATON based on the single crystal X-ray diffraction data (Table S2†).[19] Corresponding adsorption analyses of **1a–3a** are summarized in Table 1. Meanwhile, a N_2 sorption study was performed on **1a** as an example after water, HCl (pH = 2) and NaOH (pH = 12) treatment, in order to further testify the stability of MOFs. The N_2 adsorptions showed that the adsorption amount and surface area decrease (Fig. S6 and Table S3†). It can be due to the fact that water and acid/alkaline solutions destroyed the framework to a certain degree, although XRPD patterns were kept the same . Subsequently we carried out CO_2 adsorption experiments on **1a–5a**. As shown in Fig. 3, the CO_2 sorption isotherms for **1a–5a** were measured at 195, 273 and 298 K, respectively. **1a–5a** have CO_2 uptakes at 1 bar with saturation of 188.5 $cm^3\ g^{-1}$, 136.3 $cm^3\ g^{-1}$, 108.9 $cm^3\ g^{-1}$, 86.88 $cm^3\ g^{-1}$, and 70.68 $cm^3\ g^{-1}$ at 195 K, 103.7 $cm^3\ g^{-1}$, 37.7 cm^3

Table 1 Structural information and N_2 adsorption analyses

	N_2 adsorption amount ($cm^3\ g^{-1}$)	Void (%)	Pore volume ($cm^3\ g^{-1}$)	S_{BET} ($m^2\ g^{-1}$)
1a	118.5	52.0	0.212	363
2a	150.3	45.6	0.320	453
3a	158.2	46.6	0.245	506

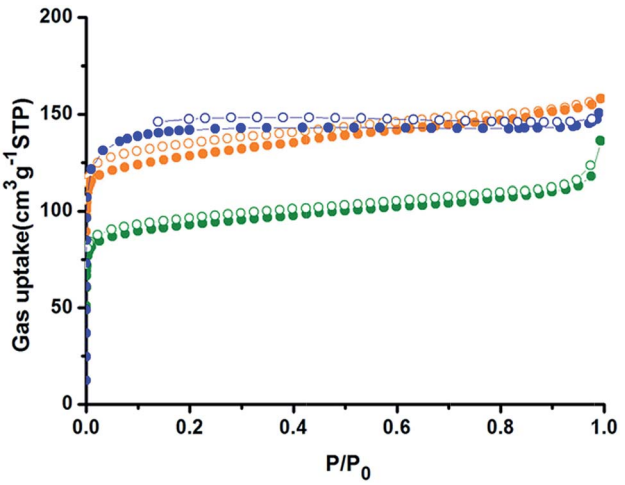

Fig. 2 The nitrogen sorption isotherms of **1a** (green), **2a** (blue) and **3a** (yellow) at 77 K.

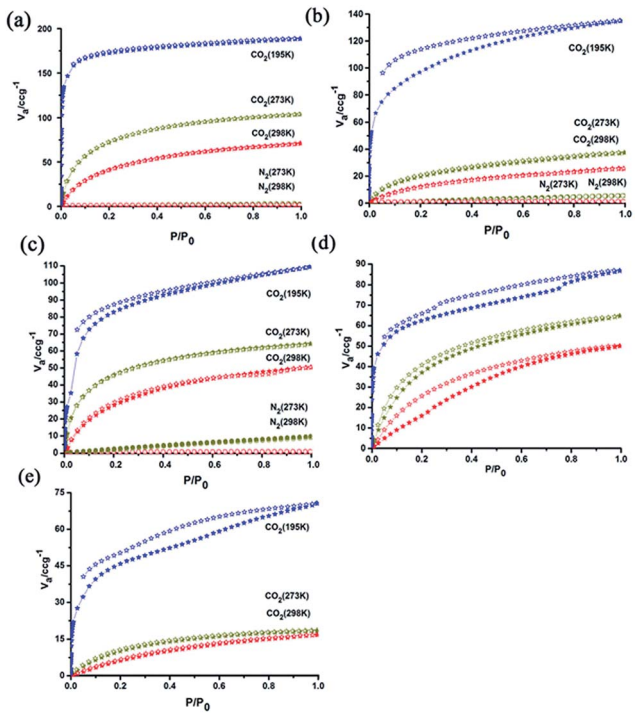

Fig. 3 CO_2 and N_2 sorption isotherms for (a) **1a**, (b) **2a**, (c) **3a**, (d) **4a** and (e) **5a** at 195, 273 and 298 K.

Table 2 CO_2 adsorption analyses for **1a–5a**

	195 K		273 K		298 K	
	$cm^3\ g^{-1}$	mmol g^{-1}	$cm^3\ g^{-1}$	mmol g^{-1}	$cm^3\ g^{-1}$	mmol g^{-1}
1a	188.5	8.42	103.7	4.63	70.2	3.13
2a	136.3	6.08	37.7	1.68	25.7	1.15
3a	108.9	4.86	63.9	2.85	50.5	2.25
4a	86.88	3.88	64.3	2.87	50.1	2.24
5a	70.68	3.16	18.6	0.83	17.2	0.77

g^{-1}, 63.9 $cm^3\ g^{-1}$, 64.3 $cm^3\ g^{-1}$, and 18.6 $cm^3\ g^{-1}$ at 273 K, and 70.2 $cm^3\ g^{-1}$, 25.7 $cm^3\ g^{-1}$, 50.5 $cm^3\ g^{-1}$, 50.1 $cm^3\ g^{-1}$, and 17.2 $cm^3\ g^{-1}$ at 298 K (Fig. 3 and Table 2). For **1–5**, the isosteric heats of adsorption (Q_{st}) of CO_2 were calculated by using the Clausius–Clapeyron equation to quantitatively evaluate the binding strengths (Fig. S8–S12†).[20] The Q_{st} at zero coverage of CO_2 of **1** was about 33 kJ mol^{-1}, thus indicating strong interactions between CO_2 and the framework. The CO_2-uptakes and enthalpy of adsorption for selected MOFs and **1** are listed in Table S4.† Unexpectedly, the CO_2 uptakes for **1a–3a** are quite high while N_2 sorption was hardly observed at 273 and 298 K (Fig. 3).

Iodine sorption

The permanent porosity of **1–5** demonstrated by N_2 sorption studies prompted us to search for absorption of some molecules.[21] Among the five isostructural compounds, we selected **1** as an example. When the fresh samples of **1** (80 mg) were immersed in a hexane (3 mL) solution of I_2 (0.01 mol L^{-1}), we observed that the color of the crystals intensified from light yellow to dark brown, while the dark brown solution of I_2 faded gradually to pale red in hours. The entry of I_2 into the **1** host framework results in a distinct decrease of the fluorescence emission intensity (λ_{ex} = 311 nm and λ_{em} = 405 nm), which may be attributed to the host–guest photoinduced electron transfer effect (Fig. S13†).[22] The decline of the fluorescence intensity also indicates that **1** can quickly adsorb iodine. When the crystals of I_2@**1** were soaked in dry ethanol, the color of the crystals changed gradually from dark brown to light yellow and the color of the ethanol solution deepened gradually from colorless to darker yellow, as represented in Fig. 4. To further investigate the kinetics of I_2 delivery of **1** in crystal transformation, the UV/vis spectrum was recorded at room temperature. The absorbance of I_2 in ethanol increases linearly with time. The releasing rate becomes slower later because the concentration of I_2 in ethanol increases with time. To verify the repeatability, the reversible I_2 sorption process was tested for two cycles. The photographs, UV and luminescent spectrum for **1** releasing I_2 demonstrate that the I_2 sorption process is reversible and repeatable (Fig. 4 and S14†).

The integrity of the framework is confirmed by the XRPD data (Fig. S15†). It is worth saying that when the crystals were soaked in the solution of I_2 for about 60 minutes, some peaks of XRPD patterns became weak, while, the peaks appeared again

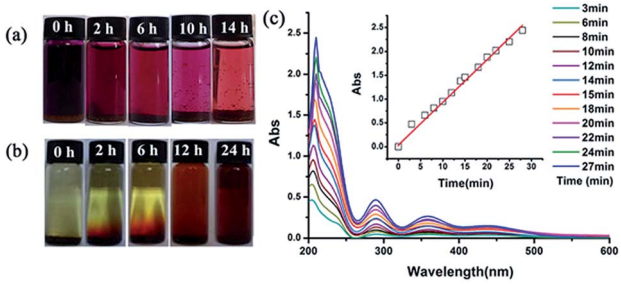

Fig. 4 (a) Photographs showing the color change when **1** (80 mg) was soaked in hexane solution of I_2 (3 mL, 0.01 mol L^{-1}). (b) The I_2 release process when I_2@**1** (50 mg) was immersed in EtOH (3 mL). (c) The UV/vis spectra of I_2@**1** for the releasing process of iodine.

when the I_2 was removed from the framework upon immersion of the crystals in ethanol. This phenomenon can be well explained by the fact that the high amount of iodine in **1** has a significant impact on the sensitivity of X-ray.

Dye sorption from aqueous solution

To investigate the abilities of **1–5** to separate dye molecules, we used them to capture dyes in water. Two types of dyes with different charges: positively charged Methylene Blue (MB) and Rhodamine B (RB), and negatively charged Methyl Orange (MO) and Congo Red (CR) were chosen as models of pollutants. Typically, when 30 mg of **1–5** were soaked in 3 mL of dye-contaminated water (2×10^{-5} mol L^{-1}), respectively, some dye molecules could be efficiently adsorbed over a period of time and the colorless crystals gradually became colored, while some dye molecules could not be incorporated (Fig. S16†). Corresponding adsorption analyses of **1–5** are summarized in Table 3.

1, **2** and **5** were designed with tunable channels by using size-alterable organic linkers, while **3** and **4** have similar interlayer distances to **2** despite different functional groups. Considering the above cases, we chose **1**, **2** and **5** for the dye molecules inclusion study. RB and MB with different sizes were selected for these experiments. When refreshed **1**, **2** and **5** were soaked in water of mixture of two kinds of dyes, different phenomena were observed. Because the pore size of **1** is smaller than that of RB and MB, scarcely any amount of absorbed dyes were detected (Fig. 5a). As shown in Fig. 5b, the continuing decrease of characteristic absorbance for MB

Table 3 The list of dye adsorption analyses of **1–5**[a]

Adsorbate/Samples	MB	MO	RB	CR
1	×	×	×	×
2	√	√	×	×
3	√	√	×	×
4	√	√	×	×
5	√	√	√	√

[a] √ = absorbed; × = excluded MB = Methylene Blue; MO = Methyl Orange; RB = Rhodamine B; CR = Congo Red.

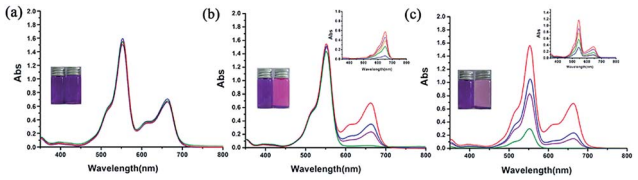

Fig. 5 Photographs and UV/vis spectra of aqueous solutions of mixtures of RB and MB dyes with (a) **1**, (b) **2** and (c) **5** (UV/vis spectra of dye releasing in MeOH are showed at the top).

reveals its successful incorporation whereas the unchanged peak of RB suggests its exclusion by the channels of **2**. This phenomenon can be ascribed to that the pore size of **2** is bigger than that of MB but smaller than that of RB, while the continuing decreases of characteristic absorbances for MB and RB reveal that **5** has the ability to incorporate these two dye molecules (Fig. 5c). The differences in adsorptions may be caused by size factors, since the sizes of channel windows are in the order of **5** > **2** > **1**. The capabilities of **1**, **2** and **5** to adsorb dyes from water were evaluated through UV/vis spectroscopy and confirmed in Fig. 5. To confirm that selective absorptions are repeatable, dye releasing experiments were performed in MeOH, measured by UV/vis spectroscopy. This showed that, the dye molecules can be gradually released because dye molecules are more easily dissolved in MeOH. The results indicate that **1–5** show excellent adsorption properties and repeatabilities.

Considering the above results in mind, **2–4** have the abilities to separate large dye molecules based on the size-exclusion effect (Table 3).[23] **3** was employed as a column-chromatographic filler for separation of RB and MB based on the size-exclusion effect. As displayed in Fig. 6, the larger and unincorporated RB was transported through the column along with the water stream while the incorporated MB was retained inside the MOF channels for longer time, thus resulting in the separation, which was not only observable by the naked eye but was also confirmed by UV/vis spectra of the effluent.

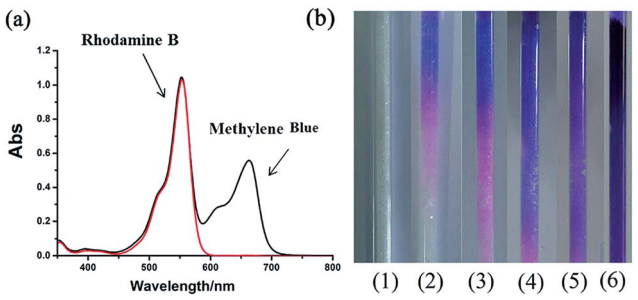

Fig. 6 (a) UV/vis spectra of the original effluent (black) and effluent passing through the MOF chromatographic column (red) of the dye mixture of RB and MB. (b) Photograph records for the **3**-filled column-chromatographic separation process for RB and MB dyes, in which (1) **3**-filled column, (2–5) separation process with gradually changed color, and (6) complete separation with only MB retained.

Conclusion

In summary, we utilized an already established and powerful approach for the targeted manipulation of an important family of pillared-layer MOFs. The resulting MOFs show similar structures but different interlayer distances, pore volumes and pore surface functionalizations depending on the length and functions of the pillar linkers. **1–5** display a certain amount of CO_2 uptake, and the CO_2 uptakes of **2** and **5** can definitely not be considered to be high. With the merit of microporosity, **1** was selected as an example to carry out the I_2 adsorption experiment which exhibited a rapidly reversible process. Interestingly, **1–5** were investigated for capturing dyes in water. They show different dye absorption capacities because of different pore volumes resulting from size-alterable ligands, and repeatabilities. Meanwhile, **3** has been demonstrated to be a column-chromatographic filler for the separation of bulk dye molecules. The synthetic strategy presents a progressive evolution for the construction of pillared-layer frameworks and the MOF materials for functional applications are currently underway.

Acknowledgements

This work was financially supported by the NSFC of China (no. 21001022, 21171033, 21131001, 21222105, 20801041), PhD Station Foundation of Ministry of Education (20100043110003), The Foundation for Author of National Excellent Doctoral Dissertation of P.R.China (FANEDD) (no. 201022), The Science and Technology Development Planning of Jilin Province (20111803).

Notes and references

1 (*a*) O. M. Yaghi, M. O'Keeffe, N. W. Ockwig, H. K. Chae, M. Eddaoudi and J. Kim, *Nature*, 2003, **423**, 705; (*b*) G. Férey, *Chem. Soc. Rev.*, 2008, **37**, 191; (*c*) M. J. Zaworotko, *Nature*, 2008, **451**, 410; (*d*) C. Volkringer, D. Popov, T. Loiseau, N. Guillou, G. Férey, M. Haouas, F. Taulelle, C. Mellot-Draznieks, M. Burghammer and C. Riekel, *Nat. Mater.*, 2007, **6**, 760; (*e*) S. J. Dalgarno, N. P. Power and J. L. Atwood, *Coord. Chem. Rev.*, 2008, **252**, 825; (*f*) M. P. Suh, Y. E. Cheon and E. Y. Lee, *Coord. Chem. Rev.*, 2008, **252**, 1007; (*g*) S. Kitagawa and R. Matsuda, *Coord. Chem. Rev.*, 2007, **251**, 2490; (*h*) X. L. Wang, C. Qin, S. X. Wu, K. Z. Shao, Y. Q. Lan, S. Wang, D. X. Zhu, Z. M. Su and E. B. Wang, *Angew. Chem.*, 2009, **121**, 5395; *Angew. Chem., Int. Ed.*, 2009, **48**, 5291.

2 (*a*) H. K. Chae, D. Y. Siberio-Perez, J. Kim, Y. B. Go, M. Eddaoudi, A. J. Matzger, M. O'Keeffe and O. M. Yaghi, *Nature*, 2004, **427**, 523; (*b*) X. Zhao, B. Xiao, A. J. Fletcher, K. M. Thomas, D. Bradshaw and M. J. Rosseinsky, *Science*, 2004, **306**, 1012; (*c*) J. A. R. Navarro, E. Barea, A. Rodriguez-Dieguez, J. M. Salas, C. O. Ania, J. B. Parra, N. Masciocchi, S. Galli and A. Sironi, *J. Am. Chem. Soc.*, 2008, **130**, 3978; (*d*) C. D. Wood, B. Tan, A. Trewin, F. Su, M. J. Rosseinsky, D. Bradshaw, Y. Sun, L. Zhou and A. I. Cooper, *Adv. Mater.*, 2008, **20**, 1916; (*e*) F. Nouar, J. F. Eubank, T. Bousquet,

L. Wojtas, M. J. Zaworotko and M. Eddaoudi, *J. Am. Chem. Soc.*, 2008, **130**, 1833.

3 (*a*) S. Horike, M. Dincă, K. Tamaki and J. R. Long, *J. Am. Chem. Soc.*, 2008, **130**, 5854; (*b*) M. Fujita, J. Y. Kwon, S. Washizu and K. Ogura, *J. Am. Chem. Soc.*, 1994, **116**, 1151; (*c*) J. S. Seo, D. Whang, H. Lee, S. I. Jun, J. Oh, Y. J. Jeon and K. Kim, *Nature*, 2000, **404**, 982; (*d*) C. D. Wu and W. Lin, *Angew. Chem., Int. Ed.*, 2007, **46**, 1075; (*e*) T. M. McDonald, W. R. Lee, J. A. Mason, B. M. Wiers, C. S. Hong and J. R. Long, *J. Am. Chem. Soc.*, 2012, **134**, 7056; (*f*) P. Horcajada, R. Gref, T. Baati, P. K. Allan, G. Maurin, P. Couvreur, G. Férey, R. E. Morris and C. Serre, *Chem. Rev.*, 2012, **112**, 1232.

4 (*a*) X. L. Hu, C. Y. Sun, C. Qin, X. L. Wang, H. N. Wang, E. L. Zhou, W. E. Li and Z. M. Su, *Chem. Commun.*, 2013, **49**, 3564; (*b*) R. Matsuda, R. Kitaura, S. Kitagawa, Y. Kubota, R. V. Belosludov, T. C. Kobayashi, H. Sakamoto, T. Chiba, M. Takata, Y. Kawazoe and Y. Mita, *Nature*, 2005, **436**, 238; (*c*) S. Ma, X. S. Wang, D. Yuan and H. C. Zhou, *Angew. Chem., Int. Ed.*, 2008, **47**, 4130; (*d*) L. Pan, D. H. Olson, L. R. Ciemnolonski, R. Heddy and J. Li, *Angew. Chem., Int. Ed.*, 2006, **45**, 616; (*e*) T. K. Maji, R. Matsuda and S. Kitagawa, *Nat. Mater.*, 2007, **6**, 142; (*f*) B. L. Chen, Y. Yang, F. Zapata, G. N. Lin, G. D. Qian and E. B. Lobkovsky, *Adv. Mater.*, 2007, **19**, 1693.

5 (*a*) S. G. Férey, C. Mellot-Draznieks, F. Millange, S. Surblé, J. Dutour and I. Margiolaki, *Angew. Chem., Int. Ed.*, 2004, **43**, 6296; (*b*) C. Mellot-Draznieks, J. Dutour and G. Férey, *Angew. Chem., Int. Ed.*, 2004, **43**, 6290; (*c*) H. L. Jiang, Y. Tatsu, Z. H. Lu and Q. Xu, *J. Am. Chem. Soc.*, 2010, **132**, 5586; (*d*) G. S. Yang, M. N. Li, S. L. Li, Y. Q. Lan, W. W. He, X. L. Wang, J. S. Qin and Z. M. Su, *J. Mater. Chem.*, 2012, **22**, 17947.

6 (*a*) A. Schoedel, W. Boyette, L. Wojtas, M. Eddaoudi and M. J. Zaworotko, *J. Am. Chem. Soc.*, 2013, **135**, 14016; (*b*) M. Eddaoudi, J. Kim, N. Rosi, D. Vodak, J. Wachter, M. O'Keeffe and O. M. Yaghi, *Science*, 2002, **295**, 469; (*c*) D. Denysenko, M. Grzywa, M. Tonigold, B. Streppel, I. Krkljus, M. Hirscher, E. Mugnaioli, U. Kolb, J. Hanss and D. Volkmer, *Chem.–Eur. J.*, 2011, **17**, 1837; (*d*) D. Yuan, D. Zhao and H. C. Zhou, *Inorg. Chem.*, 2011, **50**, 10528; (*e*) H. Furukawa, Y. B. Go, N. Ko, Y. K. Park, F. J. Uribe-Romo, J. Kim, M. O'Keeffe and O. M. Yaghi, *Inorg. Chem.*, 2011, **50**, 9147; (*f*) X. Lin, I. Telepeni, A. I. Blake, A. Dailly, C. M. Brown, J. M. Simmons, M. Zoppi, G. S. Walker, K. M. Thomas, T. J. Mays, P. Hubberstey, N. R. Champness and M. Schröder, *J. Am. Chem. Soc.*, 2009, **131**, 2159.

7 (*a*) T. J. Prior, D. Bradshaw, S. J. Teat and M. J. Rosseinsky, *Chem. Commun.*, 2003, 500; (*b*) J. L. Song, H. H. Zhao, J. G. Mao and K. R. Dunbar, *Chem. Mater.*, 2004, **16**, 1884; (*c*) Z. J. Zhang, J. C. Liu, Z. Li and J. Li, *Dalton Trans.*, 2012, **41**, 4232; (*d*) Z. Chang, D. S. Zhang, Q. Chen, R. F. Li, T. L. Hu and X. H. Bu, *Inorg. Chem.*, 2011, **50**, 7555; (*e*) I. H. Park, K. Kim, S. S. Lee and J. J. Vittal, *Cryst. Growth Des.*, 2012, **12**, 3397.

8 (*a*) H. N. Wang, X. Meng, C. Qin, X. L. Wang, G. S. Yang and Z. M. Su, *Dalton Trans.*, 2012, **41**, 1047; (*b*) D. R. Xiao, E. B. Wang, H. Y. An, Y. G. Li, Z. M. Su and C. Y. Sun, *Chem.–Eur. J.*, 2006, **12**, 6528; (*c*) M. J. Zaworotko, *Chem. Commun.*, 2001, **40**, 2111; (*d*) H. L. Ngo and W. Lin, *J. Am. Chem. Soc.*, 2002, **124**, 14298; (*e*) R. Kitaura, K. Fujimoto, S. L. Noro, M. Kondo and S. Kitagawa, *Angew. Chem., Int. Ed.*, 2002, **114**, 141; (*f*) Y. Diskin-Posner, S. Dahal and I. Goldberg, *Angew. Chem., Int. Ed.*, 2000, **112**, 1344.

9 (*a*) C. Zhang, Y. Cao, J. Zhang, S. Meng, T. Matsumoto, Y. Song, J. Ma, Z. Chen, K. Tatsumi and M. G. Humphrey, *Adv. Mater.*, 2008, **20**, 1870; (*b*) S. Horike, S. Bureekaew and S. Kitagawa, *Chem. Commun.*, 2008, 471; (*c*) T. Shiga, H. Okawa, S. Kitagawa and M. Ohba, *J. Am. Chem. Soc.*, 2006, **128**, 16426; (*d*) B. Liu, M. Ma, D. Zacher, A. Bétard, K. Yusenko, N. Metzler-Nolte, C. Wöll and R. A. Fischer, *J. Am. Chem. Soc.*, 2011, **133**, 1734.

10 (*a*) R. Matsuda, R. Kitaura, S. Kitagawa, Y. Kubota, T. C. Kobayashi, S. Horike and M. Takata, *J. Am. Chem. Soc.*, 2004, **126**, 14063; (*b*) T. K. Maji, K. Uemura, H. C. Chang, R. Matsuda and S. Kitagawa, *Angew. Chem., Int. Ed.*, 2004, **116**, 3331; (*c*) S. Henke, A. Schneemann, A. Wütscher and R. A. Fischer, *J. Am. Chem. Soc.*, 2012, **134**, 9464.

11 B. Adhikari, G. Palui and A. Banerjee, *Soft Matter*, 2009, **5**, 3452.

12 (*a*) C. Y. Sun, X. L. Wang, C. Qin, J. L. Jin, Z. M. Su, P. Huang and K. Z. Shao, *Chem.–Eur. J.*, 2013, **19**, 3639; (*b*) C. Zou, Z. J. Zhang, X. Xu, Q. H. Gong, J. Li and C. D. Wu, *J. Am. Chem. Soc.*, 2012, **134**, 87; (*c*) M. A. Al-Ghouti, M. Khraisheh, S. J. Allen and M. N. Ahmad, *J. Environ. Manage.*, 2003, **69**, 229; (*d*) L. Zhou, C. Gao and W. Xu, *ACS Appl. Mater. Interfaces*, 2010, **2**, 1483.

13 (*a*) W. X. Chen, W. Y. Lu, Y. Y. Yao and M. H. Xu, *Environ. Sci. Technol.*, 2007, **41**, 6240; (*b*) D. Mahanta, G. Madras, S. Radhakrishnan and S. Patil, *J. Phys. Chem. B*, 2008, **112**, 10153; (*c*) Y. C. He, J. Yang, W. Q. Kan and J. F. Ma, *CrystEngComm*, 2013, **15**, 848.

14 G. M. Sheldrick, *SHELXS 97, Program for Crystal Structure Analysis*, University of Göttingen, Germany, 1997.

15 (*a*) G. M. Sheldrick, *SHELXS 97, Program for Crystal Structure Refinement*, University of Göttingen, Germany, 1997; (*b*) P. van der Sluis and A. L. Spek, *Acta Crystallogr., Sect. A: Found. Crystallogr.*, 1990, **46**, 194; (*c*) A. L. Spek, *J. Appl. Crystallogr.*, 2003, **36**, 7.

16 A. L. Spek, *PLATON, A Multipurpose Crystallographic Tool*, Utrecht. University, The Netherlands, 2003.

17 (*a*) M. O'Keeffe and B. G. Hyde, *Crystal Structures I: Patterns and Symmetry*, Mineralogical Society of America, Washington, DC, 1996; (*b*) F. X. Sun, G. S. Zhu, Q. R. Fang and S. L. Qiu, *Inorg. Chem. Commun.*, 2007, **10**, 649.

18 (*a*) H. Liu, Y. G. Zhao, Z. J. Zhang, N. Nijem, Y. J. Chabal, H. P. Zeng and J. Li, *Adv. Funct. Mater.*, 2011, **21**, 4754; (*b*) J. W. Zhang, H. T. Zhang, Z. Y. Du, X. Q. Wang, S. H. Yu and H. L. Jiang, *Chem. Commun.*, 2014, **50**, 1092; (*c*) L. Mu, B. Liu, H. Liu, Y. T. Yang, C. Y. Sun and G. J. Chen, *J. Mater. Chem.*, 2012, **22**, 12246.

19 J. Park, J. R. Li, Y. P. Chen, J. Yu, A. A. Yakovenko, Z. U. Wang, L. B. Sun, P. B. Balbuena and H. C. Zhou, *Chem. Commun.*, 2012, **48**, 9995.

20 (*a*) J. S. Qin, D. Y. Du, W. L. Li, J. P. Zhang, S. L. Li, Z. M. Su, X. L. Wang, Q. Xu, K. Z. Shao and Y. Q. Lan, *Chem. Sci.*, 2012, **3**, 2114; (*b*) S. S. Kaye and J. R. Long, *J. Am. Chem. Soc.*, 2005, **127**, 6506; (*c*) J. P. Zhang and X. M. Chen, *J. Am. Chem. Soc.*, 2009, **131**, 5516.

21 (*a*) M. H. Zeng, Q. X. Wang, Y. X. Tan, S. Hu, H. X. Zhao, L. S. Long and M. Kurmoo, *J. Am. Chem. Soc.*, 2010, **132**, 2561; (*b*) Q. K. Liu, J. P. Ma and Y. B. Dong, *Chem. Commun.*, 2011, **47**, 7185; (*c*) L. Chen, K. Tan, Y. Q. Lan, S. L. Li, K. Z. Shao and Z. M. Su, *Chem. Commun.*, 2012, **48**, 5919; (*d*) J. H. Cui, Z. Z. Lu, Y. Z. Li, Z. J. Guo and H. G. Zheng, *Chem. Commun.*, 2012, **48**, 7967; (*e*) L. E. Kreno, K. Leong, O. K. Farha, M. Allendorf, R. P. Van Duyne and J. T. Hupp, *Chem. Rev.*, 2012, **112**, 1105.

22 (*a*) B. Zhao, X. Y. Chen, P. Cheng, D. Z. Liao, S. P. Yan and Z. H. Jiang, *J. Am. Chem. Soc.*, 2004, **126**, 15394; (*b*) W. W. He, S. L. Li, G. S. Yang, Y. Q. Lan, Z. M. Su and Q. Fu, *Chem. Commun.*, 2012, **48**, 10001.

23 (*a*) F. Pu, X. Liu, B. L. Xu, J. S. Ren and X. G. Qu, *Chem.–Eur. J.*, 2012, **18**, 4322; (*b*) H. L. Jiang, Y. Tatsu, Z. H. Lu and Q. Xu, *J. Am. Chem. Soc.*, 2010, **132**, 5586.